Non-coding RNA Research 9 (2024) 744–758

Contents lists available at ScienceDirect

Non-coding RNA Research

journal homepage: www.keaipublishing.com/en/journals/non-coding-rna-research

Original Research Article

Noncoding RNA-associated competing endogenous RNA networks in trastuzumab-induced cardiotoxicity

Suifen Xie [a,b,c,1], Ni Zhou [a,b,c,1], Nan Su [d], Zijun Xiao [a,b], Shanshan Wei [a,b], Yuanying Yang [a,b], Jian Liu [a,b], Wenqun Li [a,b,*], Bikui Zhang [a,b,**]

[a] Department of Pharmacy, The Second Xiangya Hospital, Central South University, Changsha, Hunan, 410011, China
[b] Institute of Clinical Pharmacy, Central South University, Changsha, Hunan, 410011, China
[c] Xiangya School of Pharmaceutical Sciences, Central South University, Changsha, Hunan, 410013, China
[d] Department of Ophthalmology, The First People's Hospital of Lanzhou City, Lanzhou, 730050, Gansu Province, China

ARTICLE INFO

Keywords:
Trastuzumab
Cardiotoxicity
Noncoding RNA
Whole transcriptome sequencing
ceRNA networks

ABSTRACT

Trastuzumab-induced cardiotoxicity (TIC) is a common and serious disease with abnormal cardiac function. Accumulating evidence has indicated certain non-coding RNAs (ncRNAs), functioning as competing endogenous RNAs (ceRNAs), impacting the progression of cardiovascular diseases. Nonetheless, the specific involvement of ncRNA-mediated ceRNA regulatory mechanisms in TIC remains elusive. The present research aims to comprehensively investigate changes in the expressions of all ncRNA using whole-transcriptome RNA sequencing. The sequencing analysis unveiled significant dysregulation, identifying a total of 43 circular RNAs (circRNAs), 270 long noncoding RNAs (lncRNAs), 12 microRNAs (miRNAs), and 4131 mRNAs in trastuzumab-treated mouse hearts. Subsequently, circRNA-based ceRNA networks consisting of 82 nodes and 91 edges, as well as lncRNA-based ceRNA networks comprising 111 nodes and 112 edges, were constructed. Using the CytoNCA plugin, pivotal genes—miR-31-5p and miR-644-5p—were identified within these networks, exhibiting potential relevance in TIC treatment. Additionally, KEGG and GO analyses were conducted to explore the functional pathways associated with the genes within the ceRNA networks. The outcomes of the predicted ceRNAs and bioinformatics analyses elucidated the plausible involvement of ncRNAs in TIC pathogenesis. This insight contributes to a better understanding of underlying mechanisms and aids in identifying promising targets for effective prevention and treatment strategies.

1. Introduction

Trastuzumab (Tra), a widely used monoclonal antibody, has been used for the treatment of breast, colorectal, and gastric cancers [1]. Its function involves inhibiting cancer cell growth and enhancing the immune system's capacity to eliminate these cells. Tra is seldom used alone but is commonly combined with chemotherapy and radiotherapy as adjuvant therapy [2]. However, its clinical application has been hampered by acute and chronic cardiotoxic side effects, know as Tra-induced cardiotoxicity (TIC) [3].

The main phenotype of TIC manifests as a diffuse decrease in left ventricular wall motion and myocardial wall thickness, resembling dilated cardiomyopathy [4]. Proven factors contributing to TIC include the release of pro-inflammatory cytokine, apoptosis, mitochondrial damage, yet, the exact mechanisms remain unclear [5,6]. Exploring strategies and biomarkers to prevent this disease is critical and urgent.

Recently, ncRNAs such as lncRNAs, miRNA, and circRNAs, characterized by covalently closed-loop structures, have garnered significant research attention. LncRNAs, except for the minimum size limit of 200 nt and a lack of protein-coding potential, exhibit considerable diversity in

Abbreviations: **ceRNAs**, Competing Endogenous RNAs; **CK**, Creatine Kinase; **cTnT**, Cardiac Troponin T; **DEGs**, Differentially Expressed Genes; **FS**, fractional Shortening; **LDH**, Lactate Dehydrogenase; **LVEF**, Left Ventricular Ejection Fraction; **MREs**, MiRNA Response Elements; **ncRNAs**, non-coding RNAs; **PCC**, Pearson Correlation Coefficient; **RBP**, RNA-bind protein; **RNA-seq**, RNA Sequencing; **TIC**, Trastuzumab-induced Cardiotoxicity; **Tra**, Trastuzumab.

* Corresponding author. Department of Pharmacy, The Second Xiangya Hospital, Central South University, Changsha, Hunan, 410011, China.
** Corresponding author. Department of Pharmacy, The Second Xiangya Hospital, Central South University, Changsha, Hunan, 410011, China.
E-mail addresses: liwq1204@csu.edu.cn (W. Li), 505995@csu.edu.cn (B. Zhang).
[1] These authors contributed equally to this work.

https://doi.org/10.1016/j.ncrna.2024.02.004
Received 17 October 2023; Received in revised form 17 January 2024; Accepted 6 February 2024
Available online 22 February 2024
2468-0540/© 2024 The Authors. Publishing services by Elsevier B.V. on behalf of KeAi Communications Co. Ltd. This is an open access article under the CC BY-NC-ND license (http://creativecommons.org/licenses/by-nc-nd/4.0/).

structural, functional, and mechanistic features, representing a highly diverse group of regulatory ncRNAs [7]. Similarly, miRNAs directly interact with partially complementary target sites located in the 3′ untranslated regions of target mRNAs and repress their expression [8]. CircRNAs regulate gene expression by influencing transcription, mRNA turnover, and translation by sponging RNA-binding proteins and miRNAs [9]. Accumulating evidence has demonstrated that ncRNAs could play diverse roles in multiple cardiovascular diseases through forming complex regulatory networks including feedback loops, ceRNA networks, co-expressed networks, and RNA-protein complexes [10–12].

Restoration or knockdown of some miRNAs could regulate the progression of TIC. For instance, Liu et al. validated the miR-497/FGF-23 axis as a potential indicator for predicting TIC in HER2-positive breast cancer patient [13]. Besides, miRNAs are gaining increasing recognition as potential molecular markers in the cardio-oncology field, supported by promising initial data linking them to cardiotoxicity in breast cancers [14]. While there isn't clear evidence implicating lncRNAs and circRNAs as direct targets in TIC regulation, these ncRNAs have close associations with other forms of cardiotoxicity [15].

Numerous researches have proposed that lncRNA, circRNA, and mRNA, competitively bind to the common binding sites of target miRNAs, thereby regulating the expression of miRNA or mRNA, a phenomenon known as ceRNA regulation [16,17]. These common binding sites are often referred to as miRNA response elements (MREs). Furthermore, ceRNA activity is contingent upon the abundance of miRNAs and ceRNAs, the binding affinity of ceRNAs to miRNAs, RNA editing, and RNA-binding proteins [17]. Imbalances within the ceRNA network can contribute to cancer development and progression, as well as inflammation, oxidative stress, and apoptosis in normal tissues. However, Milano et al. observed that miR-146a-5p mediates human cardiac-resident mesenchymal progenitor cells and secretes extracellular vesicles, which aid in preventing TIC *in vivo* [18].

The co-expression network of ncRNAs refers to the network of non-protein-coding RNA molecules involved in the regulation of gene expression in cells, reflecting the interaction and regulatory relationship between these ncRNA molecules, and their expression levels also show a certain correlation. Differential co-expression networks have been widely used to discover gene modules and hub genes in various cancers, such as ovarian cancer [19], retinoblastoma [20], and cervical cancer [21].

The RNA-binding proteins (RBP) network of ncRNAs refers to the interaction network formed between ncRNAs and RBPs. Within the cell, RNA-binding proteins regulate the fate and biological functions of target RNA by interacting with RNA molecules, including processes such as stabilization, transport, translation and degradation. There is a multi-level and multi-dimensional regulatory relationship between ncRNA and RBP. Numerous studies have shown that RBP plays a key regulatory role in cardiac regeneration [22], immune regulation [23], inflammatory diseases [24] and endocrine tumors [25].

The involvement of non-coding RNAs (ncRNAs) and ceRNA networks in the pathogenesis of TIC has yet to be fully elucidated. This present study systematically identifies differentially expressed miRNAs, lncRNAs, circRNAs, and mRNAs through RNA sequencing (RNA-seq)-based transcriptomic analysis. Our aim is to construct ceRNA networks with the anticipation of identifying potential targets for diagnosing and treating TIC.

2. Materials and methods

2.1. Animals and treatment

SPF grade C57BL/6 female mice, 6–8 weeks old and weighed 18–20 g, were provided by Laboratory Animal Center, Xiangya School of Medicine, Central South University (Changsha, China). Mice were housed at 22–24 °C with a 12 h light/dark cycle with unrestricted access to fodder and water. All the animal protocols were maintained in accordance with the National Institutes of Health guidelines and were approved by the Medicine Animal Welfare Committee of Xiangya School of Medicine (SYXK-2020/0019).

Twenty mice were randomly divided into two groups: control group (Con, n = 10) and Tra group (Tra, n = 10). Tra (Roche Holding AG, Switzerland, Cat#N7323) was intraperitoneally injected in mice (10 mg/kg/day, once every other day for 4 times). In the control group, a considerable dose of saline was assigned. One week after the last treatment, all mice were anaesthetized with pentobarbital and blood and heart samples were taken. Three of each group were randomly selected for follow-up testing.

2.2. Biochemical assay and echocardiography

Serum samples were obtained by centrifuging blood at a speed of 3000 rpm for a duration of 10 min. Biochemical parameters including cardiac troponin T (cTnT), lactate dehydrogenase (LDH), Creatine Kinase (CK) and CK-MB were measured (n = 10) by the Department of Laboratory Medicine, Second Xiangya Hospital, Central South University using automatic biochemical analyzer kits (Abbott Pharmaceutical Co., Ltd., Lake Bluff, IL, USA).

Mice were anaesthetized with 1.5% isoflurane, and couplers were applied to the left anterior thoracic region after hair removal. M-mode echocardiography was performed using a VisualSonics Vevo 2100 (VisualSonics, Canada), and 10–20 cardiac cycles were recorded (n = 10). Cardiac function parameters including left ventricular ejection fraction (LVEF%) and fractional shortening (FS%) were measured and calculated using the VevoStrain software workstation.

2.3. RNA-seq analyses

Sequencing was performed on the Illumina HiSeq 2500 platform at Genergy Biotechnology Co., Ltd. (Shanghai, China). The cDNA libraries of circRNAs, lncRNAs, and mRNAs were prepared according to the guidelines of TruSeq RNA LT Sample Prep Kit, v2 (Illumina), while the miRNAs libraries were prepared using the TruSeqmiRNA Sample Prep Kit, v2 (Illumina, San Diego, CA) following the provided guidelines. Subsequently, these libraries were sequenced on the Illumina HiSeq 3000 platform. Three samples were randomly selected from each group for sequencing, respectively.

2.4. Real-time quantitative polymerase chain reaction (RT qPCR) validation

Total RNA was isolated from the heart tissues by using the TRIzol reagent (Takara Bio, Dalian, China) according to the manufacturer's instructions. The concentration of RNA was tested by a NanoDrop spectrophotometer (Thermo Fisher Scientific). cDNA was synthesized from total RNA (1 μg) by using a PrimeScript RT reagent kit (Accurate Biology). RT qPCR was performed in a QuantStudio™ 5 Real Time qPCR system (Thermo) with SYBR Green I (Accurate Biology) by using gene-specific primers.

The quantitative primers used in the analysis were designed and synthesized by Sangon Biotech (Shanghai, China), and are shown in Table 1. Among them, the primer sequence for Rian was taken from Yu et al. [26]. ACTB (lncRNA), U6 (miRNA), GAPDH (circRNA and mRNA) and primers were employed as endogenous controls. Three of each type of RNA were randomly selected, with half up-regulated and half down-regulated.

2.5. Construction of the ceRNA network

The differential expression ncRNAs and mRNAs were screened between the control group and the TIC model group, choose three from each group. The sequences of ncRNAs were determined from the corresponding databases, respectively, with circRNAs using circbase (http:

Table 1
Primers used in quantitative real-time polymerase chain reaction.

Name	Forward	Reverse
Circ 3:135655500|135669339	ATTCCGCTATGTGTGTGAAGGC	ACGACCGTCAAACTCCAGTTAC
Circ 8:25640577|25649703	TTCAAGTGATCCCCAGCTTGAG	TGTGTTTCCCATGATCCCTTGC
Circ 13:93341756|93356079	TGACACAGAACTCAGAGCCAAG	ACATGAGCTCGAGTGCTGAAG
Circ 15:4035260|4059996	CAAGGCCCAGGAGAGTAC	GGCCATCCACTAAAGCAGTCC
Circ 8:86665691|86673069	CAGTATGCCTGGTCGTATCATCA	AAGTGTAGTGTGGTTTGGGC
Circ 1:43141698|43153254	GAGTTCCTCAAAGCAGGCCA	ATACTCGTCCAAGTGCCAGG
Arhgap26	TGGAACATAACCACCGAGGATAAGG	TGAGTCCAGTGTCCTGCTGATTTC
Rian	CTGTTGTGCCCTCCCTGGATG	CCAGCTAGGCTGTGTAAATCATC
Xist	TCTTACTCTCTCGGGGCTGGAAG	GAAATACGCCATAAAGGGTGTTGGG
RMST	ACTGACCCCACACATTAGCC	ACACACTCACAGCAACCTCTT
Gm37494	CATAGAAGGGGTGGTGGTGC	ATGGGGCTTTCATTGCTTGG
Ino80dos	TCTCACCCAGCTCCTTCAGT	GATGCCCTTTTCTGTTTCCAGT
mmu-miR-206-3p	GCGCGATGGAATGTAAGGAAGT	AGTGCAGGGTCCGAGGTATT
mmu-miR-31-5p	CGAGGCAAGATGCTGGCA	AGTGCAGGGTCCGAGGTATT
mmu-miR-138-5p	GCGAGCTGGTGTTGTGAATC	AGTGCAGGGTCCGAGGTATT
mmu-miR-2137	ATTTTGCCGGCGGGAGCC	AGTGCAGGGTCCGAGGTATT
mmu-miR-33-5p	GGGCGTGCATTGTAGTTGC	AGTGCAGGGTCCGAGGTATT
mmu-miR-136-3p	GGGCCATCATCGTCTCAAATG	AGTGCAGGGTCCGAGGTATT
Slmap	AAAGCAGCGACGACACTACA	TCCTGGGCTTCCACCAATTC
Tnfaip8	GAGATCATTCAGCGCCACCT	TTGTTGATGCCGTCGCAAAG
Mfn2	CCAGCAGGAATTGTCTGGGA	TGAGTTCGCTGTCCAACCAG
Tnpo1	TCAAGCACAGCAGTCCCAAA	GCCAGTGCAAAGAGGTTCTCA
Mipep	GGTGCCCTACTGACTTTGCT	GGGCGGCATAAAAGACCTGA
Syngr2	GGCGACCTGCTCTTCTCAG	CCAGCACACCCCAGGAAA

//www.circbase.org/), miRNAs using miRbase(https://www.mirbase.org/), and lncRNAs, and mRNA using ensemble (https://asia.ensembl.org/index.html). We utilized miRanda (www.microrna.org/microrna/home.do) to predict miRNA-binding seed sequence sites, target genes and potential MREs. Subsequently, predict the relationships between miRNA-circRNA, miRNA-lncRNA, and miRNA-mRNA pairs. The number of miRNAs that interact with the 3' untranslated region sequence of mRNA and circRNA or lncRNA were obtained.

Hypergeometric test was performed to estimate the enrichment of ceRNA pairs. To forecast the ceRNA score for each pair, we utilized shared miRNA-mRNA and miRNA-lncRNA (circRNA) pairs and computed it with the following formula: ceRNA_score = MRE_for_shared_miRNA/MRE_for_lncRNA (circRNA)_miRNA.

We obtained the Pearson correlation coefficient (PCC) and significant *P*-value for the expression of mRNA and circRNA (lncRNA) to assess the responsibility of MREs. The RNA pairs used for constructing circRNA-related ceRNA network and lncRNA-related ceRNA network were screened with the criteria of PPC≥0.5 and *P*-value<0.05.

CeRNAs networks were visualized utilizing Cytoscape software (v.3.8.2, San Diego, CA) and degreed the RNAs by CytoNCA. See Fig. 1 for the specific process.

2.6. Dual-luciferase reporter assay

siRNAs, reporter gene vectors and luciferase plasmids were constructed and transfected into $5*10^4$ HEK293T cells, which were left on a shaker at room temperature for 1 h after 24 h with PLB cell lysate according to the manufacturer's guidelines, and firefly luciferase activity

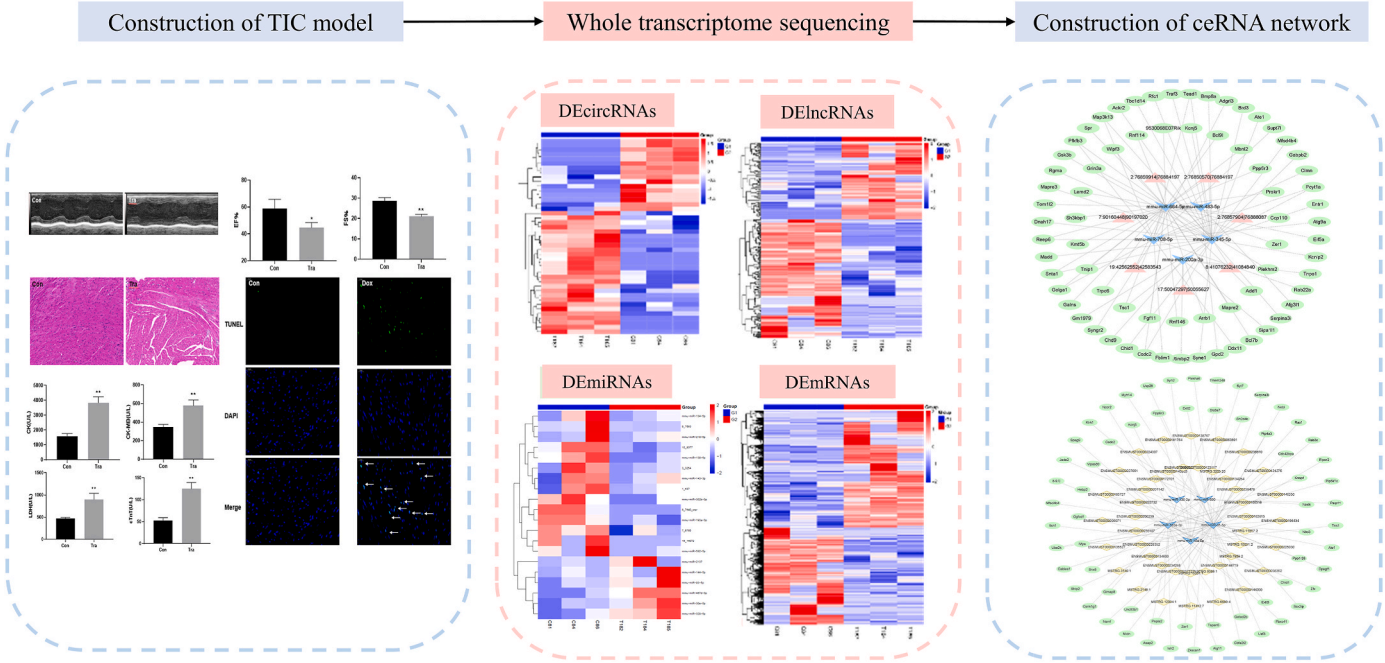

Fig. 1. The full experimental protocol and the specific flowchart of the ceRNA network construction. ceRNA, competing endogenous RNA.

was assayed by addition of LARII reagent in a multifunctional enzyme marker and normalized to Renilla luciferase activity (F/R).

2.7. GO and KEGG pathway enrichment analyses

We selected three from each group for Gene Ontology (GO) enrichment analysis and Kyoto Encyclopedia of Genes and Genomes (KEGG) pathway enrichment analysis to explored the potential functions of differentially expressed ncRNA. GO analysis was performed on the "Biological Process (BP)", "Cellular Component (CC)", and "Molecular Function (MF)" categories (www.geneontology.org). KEGG is primarily used to explore differentially expressed genes (DEGs) (www.genome.jp/kegg/).

2.8. Construction of the co-expression network

The lncRNA/circRNA-mRNA co-expression network was constructed based on expression levels in our dataset. In total, 270 lncRNAs, 43 circRNAs, 12 miRNAs, and 4131 mRNAs sensitive to Tra treatments were utilized to construct the network, employing a criterion of Spearman R $\geq$ 0.95 or $\leq$ -0.95 and a P-value<0.01. The resultant network comprised 98 lncRNAs, 9 circRNAs, 6 miRNAs, and 8 mRNAs, and its visualization was accomplished using Cytoscape.

2.9. The RNA-RBP network

The RNA-RBP network was constructed based on predicted lncRNA-RBP and circRNA-RBP interactions using RBPmap (http://rbpmap.technion.ac.il/). The lncRNA/circRNA-RBP interaction was determined by applying a criterion where the individual RNA sequence contained more than 2 motifs for the RBP of interest, selecting the two values with the highest Z-score. The RNA-RBP interactome map comprised 15 lncRNAs, 7 circRNAs, 2 miRNAs, 62 mRNAs and 79 RBPs, and was visually represented using Cytoscape.

2.10. Statistical analysis

Statistical analyses were performed by DEseq software. Histograms were constructed by GraphPad Prism 7.00. All data are presented as mean ± standard error. The expression level of each ncRNAs, and mRNAs is expressed as the logarithm of the fold change on RT qPCR analysis. mRNAs and ncRNAs were defined as differentially expressed when P < 0.05 and |log2 (fold change)|≥1. A *P*-value of<0.05 was considered statistically significant. All assays were repeated at least three times.

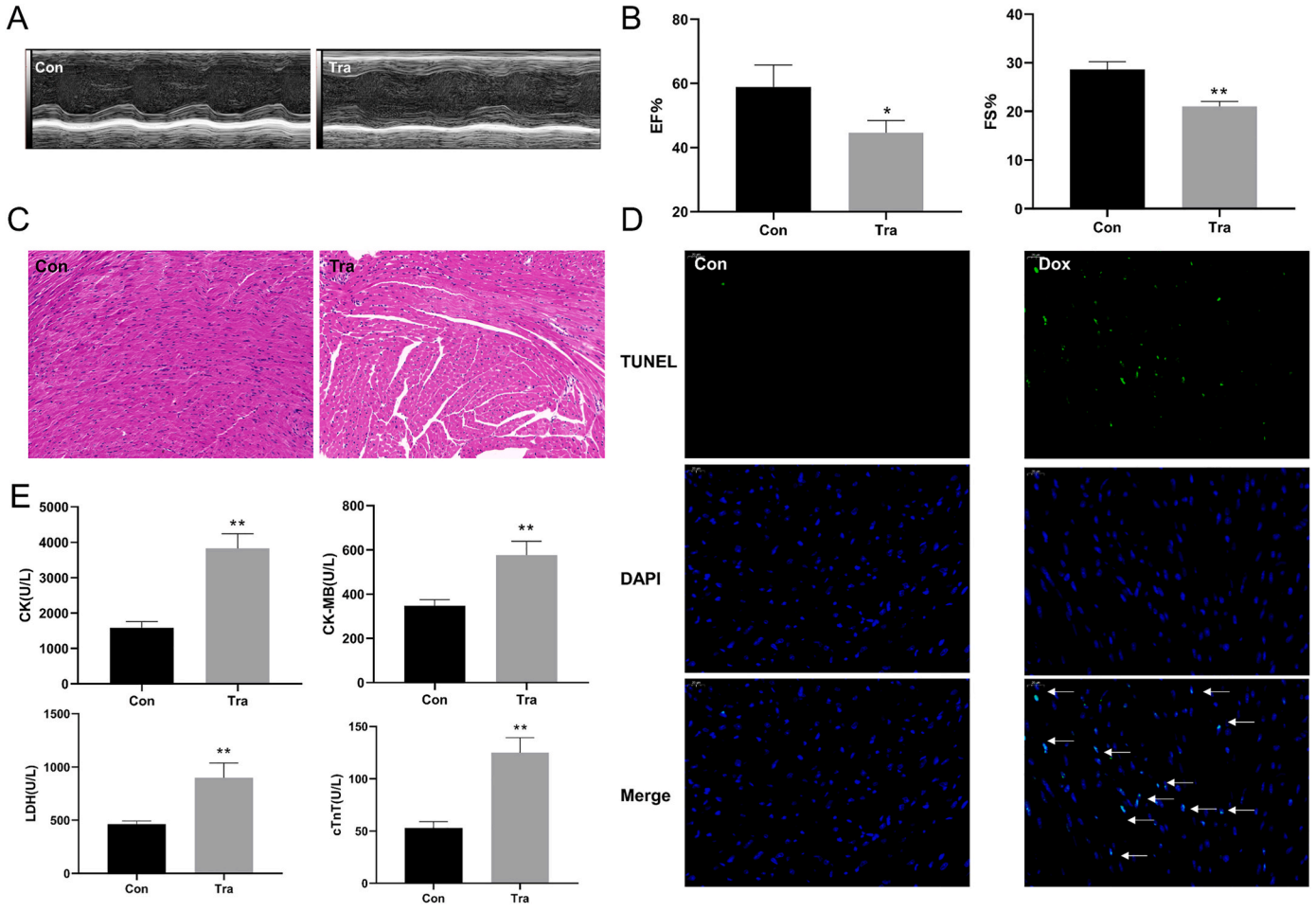

Fig. 2. Validation of the TIC model in C56BL/6 mice. (A) Echocardiography images. (B) The EF and FS of the mice were calculated. (C) Images of H&E staining. (D) Images of TUNEL staining in myocardium, nuclei of apoptotic cardiomyocytes appear in *green* fluorescence and normal nuclei appear in *blue* fluorescence. The *white* arrow points to the apoptotic cardiomyocytes. (E) Serum biochemical parameters, CK, CK-MB, LDH, and cTnT, were measured by using kits on an automated biochemical analyzer. *$P < 0.05$, **$P < 0.01$ versus Con (n = 10). TIC, trastuzumab-induced cardiotoxicity; cTnT, cardiac troponin T; LDH, lactate dehydrogenase; CK, creatine kinase; CK-MB, an isoenzyme of CK; EF, ejection fraction; FS, fractional shortening.

3. Results

3.1. Trastuzumab-induced cardiotoxicity model evaluation

We established a Trastuzumab-induced cardiotoxicity (TIC) model using 20 mice, as outlined in the methodology section. Echocardiographic assessments were performed to evaluate left ventricular systolic function (Fig. 2A). Our findings revealed a significant decrease in both LVEF% and FS% in the Tra group compared to the Con group (Fig. 2B). Moreover, histopathological examination unveiled marked tissue alterations: while the Con group exhibited normal morphology, myocardial tissues treated with Tra displayed severe disruption in myocyte structure and interstitial edema (Fig. 2C).

Additionally, a substantial increase in TUNEL staining-positive cells in cardiac tissue indicates cardiomyocyte apoptosis (Fig. 2D). As shown in Fig. 2E, the concentrations of myocardial enzyme markers in the Tra group including CK, CK-MB, LDH, and cTnT were higher than those without giving Tra, suggesting a severe cardiac injury.

3.2. Full transcriptome sequencing and differential RNA identification

Full transcriptome sequencing was performed, to estimate the expression levels of ncRNA and mRNA based on fragments per kilobase of exon per million fragments mapped and then distinguish differential expression (DE) of ncRNA and mRNA. All of the DE-RNA was filtered with set criteria and showing 43 11(Supplementary Table S1), 270 DElncRNAs (Supplementary Table S2), 12 DEmiRNAs (Supplementary Table S3) and 4131 DEmRNAs (Supplementary Table S4) on the heatmaps (Fig. 3). What's more, Table 2 lists the specific information of upregulated and downregulated DEGs and the recognized DEGs with the most and least differences.

3.3. RT-qPCR verification

RT-qPCR was used to assess the dependability of RNA-seq data, so we selected three differentially expressed transcripts of miRNA, mRNA, circRNA, and lncRNA that were up-regulated and down-regulated respectively for verification. The results of RT-qPCR showed the

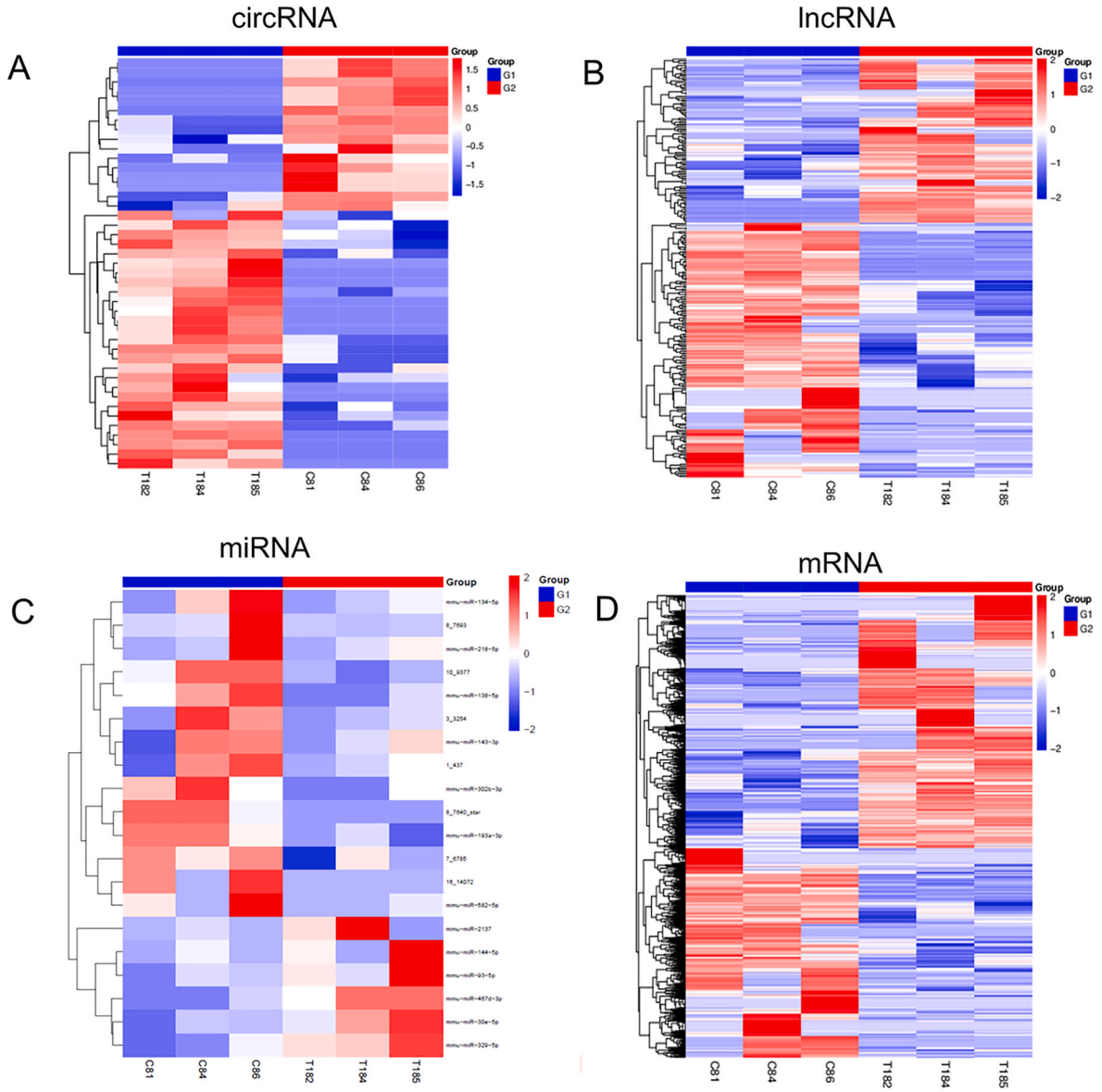

Fig. 3. Expression profiles of circRNAs, lncRNAs, miRNAs, and mRNAs. Heatmap of the expression profiles of significantly differentially expressed circRNA (A), lncRNA (B), miRNA (C), and mRNA (D) between the control group and model group. *Red* indicates increased expression, and *blue* represents decreased expression (n = 3). circRNAs, circular RNAs; lncRNA, long noncoding RNA; miRNA, microRNA.

Table 2
Statistical analysis of all differential expressed noncoding RNAs and mRNAs.

Differential expression RNAs	*Total no.*	*No. upregulated*	*No. downregulated*	*Most upregulated (log2 fold change)*	*Most downregulated (log2 fold change)*
circRNA	11503	5518	5984	12:4961218|5006791 (2.83)	14:79009164|79026077 (−2.84)
lncRNA	270	106	164	MSTRG.6223.1 (7.26)	B130046B21Rik (−5.52)
miRNA	1156	432	578	17_14928 (4.44)	18_15424 (−1.82)
mRNA	4131	1866	2265	Cnot1 (9.64)	Hnrnpu (−10.68)

circRNA, circular RNA; lncRNA, long noncoding RNA; miRNA, microRNA.

variation trend of DEGs in accordance with the RNA sequencing, demonstrating that the sequencing data were compelling (Fig. 4).

3.4. Construction of the ceRNA regulatory network

According to our previous research and the ceRNA hypothesis, we scrutinized DEmiRNAs were investigated for potential enrichment within the 'predicted mRNA and lncRNA co-binding miRNAs' set. Subsequently, we identified ceRNAs (circRNAs, lncRNAs, and mRNAs) engaged in competition for MicroRNA Response Elements (MREs) to construct ceRNA networks associated with lncRNAs or circRNAs. The visualization of these networks was achieved using Cytoscape (Fig. 5). All of the circRNAs, lncRNAs, and mRNAs predicted as MRE targets met the criteria of PPC>0.5, $p > 0.05$.

The circRNA-associated ceRNA network contains 7 circRNA, 5 miRNA and 70 mRNA, establishing 12 circRNA-miRNA interactions and 79 circRNA-mRNA interactions (Supplementary Table S5). A total of 1569 competitive regulations were associated with lncRNA, miRNA and mRNA (Supplementary Table S6). We selected 5 miRNAs exhibiting the most pronounced differential expression based on *P* value, and constructed lncRNA-associated ceRNA network in Cytoscape, incorporating mmu-miR-10a-5p, mmu-miR-690, mmu-miR-136-3p, mmu-miR-31-5p, mmu-miR-193a-3p respectively (Table 3). This network comprised 43 lncRNA, 5 miRNA, 63 mRNA, 46 lncRNA-miRNA interactions, and 67 miRNA-mRNA interactions, visualized in Fig. 5B. Notably, mmu-miR-664-5p (degree = 35) within the circRNA-associated ceRNA network and mmu-miR-31-5p (degree = 53) within the lncRNA-associated ceRNA network exhibited the highest scores, suggesting their roles as core MREs (Table 4 and Supplementary Table S6&S7). Fig. 5C and D depict sub-networks encompassing all competitive relations associated with miR-31-5p and miR-644-5p, providing further insights, details in Tables 3 and 4

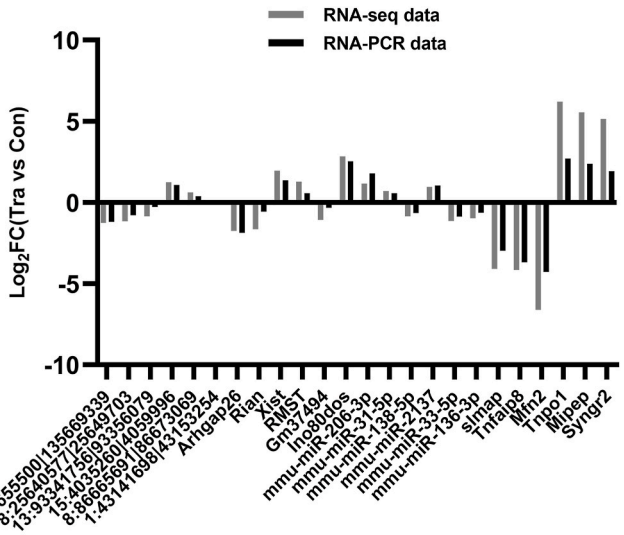

Fig. 4. The DE levels of lncRNAs, circRNAs, miRNAs, and mRNAs were validated by RT-qPCR. The expression levels of circRNAs (3:135655500|135669339, 8:25640577|25649703, 13:93341756|93356079), lncRNAs (Arhgap26, Rian, Xist), miRNAs (miR-206-3p, miR-31-5p, and miR-138-5p), and mRNAs (Slmap, Tnfaip8, Mfn2) detected by RNA-seq were consistent with RT-qPCR results (n = 6–10). DE, differential expression; RT-qPCR, real-time quantitative polymerase chain reaction; RNA-seq, RNA sequencing.

In order to confirm the ceRNA regulation, we performed a dual-luciferase reporter assay in HEK293T cells. We selected two circRNA/lncRNA-miRNA-mRNA axis with the largest score in the circRNA/lncRNA associated ceRNA network respectively for verification. Our results showed that knockdown of circRNA (Tnt) and lncRNA (Gm29683) decreased their competitive binding with miRNA (miR-345-5p/miR-193a-3p), leading to the increased binding between miRNA with mRNA (KCNJ5/Vipas39) (Fig. 5E and F). It's indicated that circRNA and lncRNA probably play their own functions through ceRNA network, but more experiments are needed to verify ceRNA regulatory mechanism if further judgment is to be made.

3.5. Enrichment analysis

To decipher the cardiac protection function of the mRNA involved in the circRNA- or lncRNA-associated ceRNA network, we executed GO and KEGG pathway enrichment analyses respectively. Using enrichment analysis, we can summarize the many different genes that look messy into a summary sentence that compares the overall response to events.

GO analysis enriched a total of 538 terms in the circRNA-associated ceRNA network and 1338 terms in the lncRNA-associated ceRNA network, and the top terms of BP, CC, and MF were individually listed in Fig. 6A&C. Among these, the most magnificent terms in the circRNA-associated ceRNA network were "the membrane repolarization", "regulation of protein binding", and "regulation of molecular function", and the top3 terms in lncRNA-associated ceRNA network were "actin filament-based process", "cellular protein modification process", and "protein modification process".

KEGG pathway maps represent metabolic processes, environmental information processes, cellular processes, biological systems, and human disease and drug development, among others. According to the KEGG enrichment results, "hippo signaling pathway" and "axon guidance" were enriched in the circRNA-associated ceRNA and lncRNA-associated ceRNA networks respectively (Fig. 6B&D).

3.6. Co-expression network for lncRNA/circRNA/miRNA/mRNA

By constructing a co-expression network of non-coding RNAs, researchers can unveil interactions, regulatory network structures, and functional insights among non-coding RNAs, aiding a deeper understanding of the intricacies of gene regulation within cells. Hence, the co-expression patterns of common DEGs were analyzed separately according to our RNA-seq data (Fig. 7A).

The co-expression network diagram comprises a total of 24 lncRNAs, 7 circRNAs, 2 miRNA, and 8 mRNAs, interconnected by 46 edges. In this representation, red nodes denote upregulated genes, while blue nodes signify downregulated genes. The findings indicate that mmu-miR-33-5p and ENSMUST00000190825 (Rbbp5) achieved the highest scores.

3.7. RNA-RBP interaction network

RNA-protein interaction represents another functional mechanism of

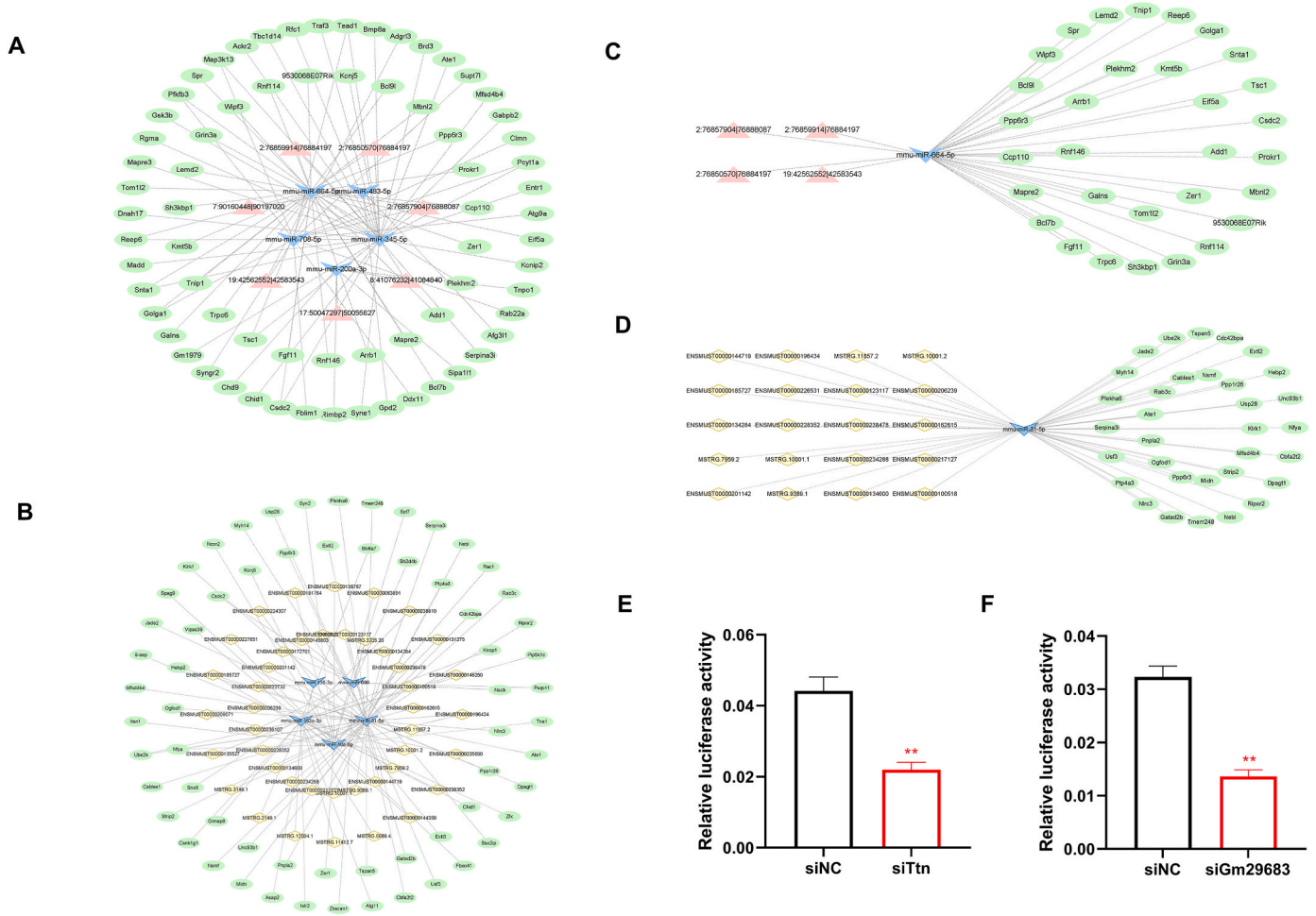

Fig. 5. circRNA-associated ceRNA networks in TIC mice and lncRNA-associated ceRNA networks in TIC mice. (A) circRNA-associated ceRNA networks in TIC mice. (B) lncRNA-associated ceRNA networks in TIC mice. Square nodes represent circRNAs, triangular nodes represent miRNAs, diamond nodes represent lncRNAs, and circular frames represent mRNAs. Red represents upregulated expression, and green indicates downregulated expression (n = 3). (C) the subnetwork of circRNA-associated ceRNA networks. (D) the subnetwork of lncRNA-associated ceRNA network. (E) and (F) the results of double luciferase experiment. HEK293T cells were transfected with sicircTtn or silncGm29683, the Renilla luciferase plasmid and Firefly luciferase reporter plasmids harboring the KCNJ5 or Vipas39 3′ UTR. The ratio of Firefly (F) to Renilla (R) in relative luciferase activity was plotted. siNC, siRNA with scrambled sequences; sicircTtn, siRNA against the junction sites of circTtn; silncGm29683, siRNA against lncGm29683. Data are representative of three independent experiments and shown as mean ± SEM. $^{**}P < 0.01$ by two-tailed Student's t-test.

RNAs. Understanding these networks contributes to the investigation of the role of RBPs in the occurrence and development of diseases. To achieve this, we constructed an RNA-RBP network (Fig. 7B). This RNA-RBP network comprises 15 lncRNAs, 7 circRNAs, 2 miRNAs, 62 mRNAs, and a predicted set of 79 RBPs. In order to delve deeper into these RBPs, we conducted KEGG and GO enrichment analyses. The results indicate a significant enrichment in RNA binding, spliceosome, and ferroptosis pathways (Fig. 7C–D).

4. Discussion

Despite its remarkable efficacy in HER-2-positive breast cancer treatment, Tra administration can present challenges linked to heart failure and diminished left ventricular contractile function [5]. In the landmark study by Slamon et al., 27% of patients treated with combinations of anthracyclines and trastuzumab developed cardiac dysfunction and 16% developed symptomatic heart failure. In comparison, only 8% and 3% of patients treated solely with an anthracycline encountered these respective issues [27]. Consequently, there exists an urgent need to determine the pharmacological mechanism underlying TIC.

Recent investigations highlight the indispensable role of ncRNAs in gene regulation across developmental processes, general health, and cardiovascular diseases. NcRNAs have been identified as critical novel regulators of cardiovascular risk factors and cellular functions, holding substantial promise for enhanced diagnostics and prognostic assessment. Moreover, ncRNAs are rapidly emerging as fundamentally novel therapeutics [28]. Consequently, our focus has shifted toward exploring alterations in ncRNAs associated with TIC.

To explore this question, we established a TIC model, revealing notable left ventricular cardiac dysfunction characterized by a significant reduction in both left ventricular ejection fraction (LVEF) and left ventricular fractional shortening (LVFS). Moreover, there was a substantial elevation in myocardial injury markers including LDH, CK, CK-MB and cTnT. Additionally, histological assessments via HE staining and TUNEL staining indicated myocardial disruption and increased myocardial apoptosis induced by Tra.

Based on the successful construction of the TIC model, we performed a whole-transcriptome RNA-seq to obtain the DE-RNAs associated with TIC including 43 DEcircRNAs, 270 DElncRNAs, 12 DEmiRNAs and 4131 DEmRNAs. Notably, several of these DEGs have been previously implicated in cardiovascular disease. For example, miR-206-3p has been linked to myocardial hypertrophy and heart failure [29]. Meanwhile,

Table 3
lncRNA-associated competing endogenous RNA network in TIC.

LncRNA	mRNA	Shared miRNAs	ceRNA score	*P*-value
ENSMUST00000196434	Kcnj5	mmu-miR-10a-5p	0.604	0.042
ENSMUST00000131275	Kcnj5	mmu-miR-10a-5p	0.683	0.021
ENSMUST00000063891	Kcnj5	mmu-miR-10a-5p	0.603	0.043
ENSMUST00000138767	Nfya	mmu-miR-10a-5p	0.587	0.048
ENSMUST00000181764	Nfya	mmu-miR-10a-5p	0.660	0.026
ENSMUST00000138767	Zer1	mmu-miR-10a-5p	0.728	0.013
ENSMUST00000227651	Zer1	mmu-miR-10a-5p	0.724	0.014
ENSMUST00000131275	Fbxo41	mmu-miR-10a-5p	0.704	0.017
ENSMUST00000209071	Rac1	mmu-miR-10a-5p	0.701	0.018
ENSMUST00000131275	Syt7	mmu-miR-10a-5p	0.599	0.044
ENSMUST00000138767	Spag9	mmu-miR-10a-5p	0.776	0.007
ENSMUST00000209071	Kcnj5	mmu-miR-10a-5p	0.960	0.000
ENSMUST00000185727	Zer1	mmu-miR-10a-5p	0.745	0.011
ENSMUST00000209071	Itsn1	mmu-miR-10a-5p	0.640	0.032
ENSMUST00000185727	Tns1	mmu-miR-10a-5p, mmu-miR-150-5p	0.647	0.030
MSTRG.3149.1	Syn2	mmu-miR-10a-5p, mmu-miR-150-5p	0.758	0.009
ENSMUST00000185727	Tns1	mmu-miR-10a-5p, mmu-miR-150-5p	0.864	0.001
MSTRG.10001.2	Kcnj5	mmu-miR-10a-5p, mmu-miR-345-5p	0.824	0.003
MSTRG.10001.2	Ncor2	mmu-miR-10a-5p, mmu-miR-345-5p	0.600	0.044
MSTRG.10001.2	Fbxo41	mmu-miR-10a-5p, mmu-miR-669c-3p, mmu-miR-708-5p	0.659	0.027
ENSMUST00000224307	Asap2	mmu-miR-136-3p	0.877	0.001
ENSMUST00000224307	Extl3	mmu-miR-136-3p	0.628	0.035
ENSMUST00000135527	8-Sep	mmu-miR-193a-3p	0.727	0.013
MSTRG.2149.1	8-Sep	mmu-miR-193a-3p	0.749	0.010
MSTRG.12004.1	Ube2k	mmu-miR-193a-3p	0.990	0.000
MSTRG.11412.7	Csnk1g1	mmu-miR-193a-3p	0.765	0.008
MSTRG.6689.4	Islr2	mmu-miR-193a-3p	0.760	0.009
ENSMUST00000144350	Islr2	mmu-miR-193a-3p	0.642	0.031
ENSMUST00000238352	Islr2	mmu-miR-193a-3p	0.596	0.045
ENSMUST00000225030	Chid1	mmu-miR-193a-3p	0.590	0.047
ENSMUST00000146250	Knop1	mmu-miR-193a-3p	0.750	0.010
MSTRG.11412.7	Vipas39	mmu-miR-193a-3p	0.616	0.039
MSTRG.12004.1	Vipas39	mmu-miR-193a-3p	0.770	0.008
MSTRG.12004.1	Vipas39	mmu-miR-193a-3p	0.990	0.000
ENSMUST00000225030	Gimap8	mmu-miR-193a-3p	0.638	0.032
ENSMUST00000238810	Gimap8	mmu-miR-193a-3p	0.696	0.019
MSTRG.2149.1	Alg11	mmu-miR-193a-3p	0.589	0.048
MSTRG.12004.1	Islr2	mmu-miR-193a-3p	0.956	0.000
ENSMUST00000146250	Zfx	mmu-miR-193a-3p	0.666	0.025
MSTRG.11412.7	Pip5k1c	mmu-miR-193a-3p	0.818	0.004
MSTRG.10001.2	Slc6a7	mmu-miR-193a-3p, mmu-miR-345-5p	0.613	0.040
MSTRG.11857.2	Ube2k	mmu-miR-31-5p	0.643	0.031
ENSMUST00000100518	Jade2	mmu-miR-31-5p	0.761	0.009
ENSMUST00000134284	Jade2	mmu-miR-31-5p	0.583	0.050
ENSMUST00000123117	Jade2	mmu-miR-31-5p	0.648	0.029
ENSMUST00000226531	Jade2	mmu-miR-31-5p	0.698	0.018
ENSMUST00000226531	Nfya	mmu-miR-31-5p	0.665	0.025
ENSMUST00000185727	Cables1	mmu-miR-31-5p	0.588	0.048
ENSMUST00000134284	Nsmf	mmu-miR-31-5p	0.855	0.002
ENSMUST00000123117	Nsmf	mmu-miR-31-5p	0.744	0.011
ENSMUST00000196434	Nsmf	mmu-miR-31-5p	0.700	0.018
ENSMUST00000201142	Tspan5	mmu-miR-31-5p	0.632	0.034
ENSMUST00000206239	Ppp1r26	mmu-miR-31-5p	0.786	0.006
ENSMUST00000228352	Cdc42bpa	mmu-miR-31-5p	0.892	0.001
ENSMUST00000134600	Cdc42bpa	mmu-miR-31-5p	0.702	0.018
ENSMUST00000234288	Cdc42bpa	mmu-miR-31-5p	0.592	0.046
ENSMUST00000217127	Cdc42bpa	mmu-miR-31-5p	0.585	0.049
ENSMUST00000228352	Extl2	mmu-miR-31-5p	0.704	0.017
ENSMUST00000134600	Extl2	mmu-miR-31-5p	0.837	0.002
MSTRG.10001.1	Extl2	mmu-miR-31-5p	0.632	0.034
MSTRG.9389.1	Extl2	mmu-miR-31-5p	0.705	0.017
ENSMUST00000206239	Hebp2	mmu-miR-31-5p	0.777	0.007
ENSMUST00000144719	Hebp2	mmu-miR-31-5p	0.749	0.010
ENSMUST00000206239	Unc93b1	mmu-miR-31-5p	0.622	0.037
ENSMUST00000228352	Cbfa2t2	mmu-miR-31-5p	0.782	0.006

(*continued on next page*)

Table 3 (*continued*)

LncRNA	mRNA	Shared miRNAs	ceRNA score	*P*-value
ENSMUST00000134600	Cbfa2t2	mmu-miR-31-5p	0.918	0.000
MSTRG.7959.2	Dpagt1	mmu-miR-31-5p	0.588	0.048
ENSMUST00000134284	Dpagt1	mmu-miR-31-5p	0.715	0.015
ENSMUST00000123117	Dpagt1	mmu-miR-31-5p	0.629	0.035
ENSMUST00000162615	Dpagt1	mmu-miR-31-5p	0.648	0.030
ENSMUST00000238478	Dpagt1	mmu-miR-31-5p	0.663	0.026
ENSMUST00000217127	Ripor2	mmu-miR-31-5p	0.617	0.038
ENSMUST00000100518	Nebl	mmu-miR-31-5p	0.603	0.043
MSTRG.9389.1	Tmem248	mmu-miR-31-5p	0.748	0.010
ENSMUST00000234288	Usp28	mmu-miR-31-5p	0.775	0.007
ENSMUST00000217127	Usp28	mmu-miR-31-5p	0.742	0.011
ENSMUST00000185727	Klrk1	mmu-miR-31-5p	0.732	0.012
ENSMUST00000228352	Klrk1	mmu-miR-31-5p	0.585	0.049
MSTRG.10001.2	Usp28	mmu-miR-31-5p	0.718	0.015
ENSMUST00000206239	Mfsd4b4	mmu-miR-31-5p	0.796	0.005
ENSMUST00000144719	Mfsd4b4	mmu-miR-31-5p	0.602	0.043
MSTRG.10001.2	Strip2	mmu-miR-31-5p	0.785	0.006
MSTRG.11857.2	Midn	mmu-miR-31-5p	0.696	0.019
ENSMUST00000228352	Cdc42bpa	mmu-miR-31-5p	0.750	0.010
ENSMUST00000234288	Gatad2b	mmu-miR-31-5p	0.657	0.027
ENSMUST00000206239	Nlrc3	mmu-miR-31-5p	0.663	0.026
ENSMUST00000162615	Nlrc3	mmu-miR-31-5p	0.587	0.048
ENSMUST00000238478	Nlrc3	mmu-miR-31-5p	0.713	0.015
ENSMUST00000206239	Ptp4a3	mmu-miR-31-5p	0.711	0.016
MSTRG.11857.2	Ptp4a3	mmu-miR-31-5p	0.676	0.023
MSTRG.9389.1	Ptp4a3	mmu-miR-31-5p	0.592	0.046
ENSMUST00000134600	Ppp6r3	mmu-miR-31-5p	0.727	0.013
ENSMUST00000234288	Ppp6r3	mmu-miR-31-5p	0.807	0.004
MSTRG.7959.2	Ogfod1	mmu-miR-31-5p	0.661	0.026
ENSMUST00000228352	Pnpla2	mmu-miR-31-5p	0.797	0.005
ENSMUST00000134600	Pnpla2	mmu-miR-31-5p	0.753	0.010
ENSMUST00000234288	Pnpla2	mmu-miR-31-5p	0.667	0.025
ENSMUST00000206239	Usf3	mmu-miR-31-5p	0.656	0.027
ENSMUST00000196434	Usf3	mmu-miR-31-5p	0.683	0.021
ENSMUST00000162615	Usf3	mmu-miR-31-5p	0.779	0.007
ENSMUST00000234288	Ate1	mmu-miR-31-5p	0.720	0.014
ENSMUST00000201142	Rab3c	mmu-miR-31-5p	0.583	0.050

Table 3 (*continued*)

LncRNA	mRNA	Shared miRNAs	ceRNA score	*P*-value
ENSMUST00000100518	Nsmf	mmu-miR-31-5p	0.620	0.037
ENSMUST00000206239	Plekha6	mmu-miR-31-5p	0.779	0.007
ENSMUST00000134284	Plekha6	mmu-miR-31-5p	0.623	0.037
ENSMUST00000162615	Plekha6	mmu-miR-31-5p	0.852	0.002
ENSMUST00000196434	Ate1	mmu-miR-31-5p	0.698	0.018
ENSMUST00000226531	Ate1	mmu-miR-31-5p	0.817	0.004
ENSMUST00000228352	Myh14	mmu-miR-31-5p	0.737	0.012
ENSMUST00000134600	Myh14	mmu-miR-31-5p	0.679	0.022
MSTRG.9389.1	Myh14	mmu-miR-31-5p	0.724	0.014
ENSMUST00000134600	Ppp6r3	mmu-miR-31-5p	0.587	0.048
ENSMUST00000234288	Ppp6r3	mmu-miR-31-5p	0.762	0.008
MSTRG.10001.1	Mfsd4b4	mmu-miR-31-5p, mmu-miR-329-3p, mmu-miR-345-5p	0.612	0.040
MSTRG.10001.2	Serpina3i	mmu-miR-31-5p, mmu-miR-345-5p	0.871	0.001
ENSMUST00000228352	Ppp6r3	mmu-miR-31-5p, mmu-miR-664-5p	0.724	0.014
ENSMUST00000217127	Ppp6r3	mmu-miR-31-5p, mmu-miR-664-5p	0.682	0.022
ENSMUST00000134284	Usf3	mmu-miR-31-5p, mmu-miR-664-5p, mmu-miR-669c-3p	0.891	0.001
MSTRG.10001.2	Ogfod1	mmu-miR-31-5p, mmu-miR-669c-3p	0.621	0.037
ENSMUST00000217127	Rab3c	mmu-miR-31-5p, mmu-miR-669c-3p	0.686	0.021
MSTRG.10001.1	Hebp2	mmu-miR-31-5p, mmu-miR-708-5p	0.594	0.046
MSTRG.3205.20	Nadk	mmu-miR-690	0.599	0.044
ENSMUST00000145803	Sh2d4b	mmu-miR-690	0.740	0.011
ENSMUST00000172701	Csdc2	mmu-miR-690	0.745	0.011
ENSMUST00000172701	Snx8	mmu-miR-690	0.590	0.047
ENSMUST00000172701	Zkscan1	mmu-miR-690	0.638	0.032
ENSMUST00000145803	Ssx2ip	mmu-miR-690	0.730	0.013
ENSMUST00000222732	Parp11	mmu-miR-690	0.671	0.024
ENSMUST00000236107	Parp11	mmu-miR-690	0.590	0.047

Ziping Song et al. demonstrated that MFN2 overexpression attenuated cardiomyocyte necroptosis via the MAM-CaMKIIδ pathway [30]. Additionally, Yuqiong Chen et al. found that rhapontigenin attenuated cardiac microvascular injury in diabetes via the inhibition of mitochondria-associated ferroptosis through the Prdx2/mfn2/acsl4 pathway [31]. Collectively, these research results indicate that the DEGs

Table 4
CircRNA-associated competing endogenous RNA network in TIC.

circRNA	mRNA	Shared miRNAs	ceRNA score	*P*-value
17:50047297|50055627	Chd9	mmu-miR-200a-3p	0.78	0.007
8:41076232|41084840	Rimbp2	mmu-miR-200a-3p	0.60	0.044
17:50047297|50055627	Rimbp2	mmu-miR-200a-3p	0.76	0.009
17:50047297|50055627	Sipa1l1	mmu-miR-200a-3p	0.63	0.035
17:50047297|50055627	Tnpo1	mmu-miR-200a-3p	0.89	0.001
2:76857904|76888087	Entr1	mmu-miR-345-5p	0.59	0.046
2:76850570|76884197	Entr1	mmu-miR-345-5p	0.79	0.006
2:76857904|76888087	Gabpb2	mmu-miR-345-5p	0.59	0.047
2:76859914|76884197	Ate1	mmu-miR-345-5p	0.74	0.011
8:41076232|41084840	Bmp8a	mmu-miR-345-5p	0.81	0.004
2:76850570|76884197	Traf3	mmu-miR-345-5p	0.58	0.049
2:76857904|76888087	Rfc1	mmu-miR-345-5p	0.67	0.024
2:76859914|76884197	Rfc1	mmu-miR-345-5p	0.70	0.019
2:76859914|76884197	Ackr2	mmu-miR-345-5p	0.87	0.001
2:76859914|76884197	Pfkfb3	mmu-miR-345-5p	0.78	0.006
2:76857904|76888087	Rgma	mmu-miR-345-5p	0.60	0.044
2:76859914|76884197	Rgma	mmu-miR-345-5p	0.77	0.007
2:76857904|76888087	Dnah17	mmu-miR-345-5p	0.85	0.002
2:76859914|76884197	Dnah17	mmu-miR-345-5p	0.77	0.008
2:76857904|76888087	Madd	mmu-miR-345-5p	0.79	0.005
2:76850570|76884197	Gm1979	mmu-miR-345-5p	0.73	0.013
8:41076232|41084840	Chid1	mmu-miR-345-5p	0.67	0.023
2:76850570|76884197	Syne1	mmu-miR-345-5p	0.63	0.035
8:41076232|41084840	Serpina3i	mmu-miR-345-5p	0.62	0.037
2:76850570|76884197	Kcnip2	mmu-miR-345-5p	0.85	0.002
2:76859914|76884197	Pcyt1a	mmu-miR-345-5p	0.72	0.015
2:76850570|76884197	Mfsd4b4	mmu-miR-345-5p	0.71	0.015
2:76859914|76884197	Brd3	mmu-miR-345-5p	0.63	0.034
2:76859914|76884197	Tead1	mmu-miR-345-5p	0.90	0.000
2:76857904|76888087	Kcnj5	mmu-miR-345-5p	0.74	0.012
2:76859914|76884197	Kcnj5	mmu-miR-345-5p	0.94	0.000
2:76850570|76884197	Tbc1d14	mmu-miR-345-5p	0.59	0.046
2:76857904|76888087	Pcyt1a	mmu-miR-345-5p	0.62	0.037
2:76859914|76884197	Map3k13	mmu-miR-345-5p	0.86	0.002
2:76859914|76884197	Gsk3b	mmu-miR-345-5p	0.65	0.029
2:76857904|76888087	Mapre3	mmu-miR-345-5p	0.78	0.007
2:76850570|76884197	Mapre3	mmu-miR-345-5p	0.72	0.014
2:76859914|76884197	Reep6	mmu-miR-345-5p, mmu-miR-664-5p	0.69	0.020
2:76857904|76888087	Reep6	mmu-miR-345-5p, mmu-miR-664-5p	0.70	0.019
2:76859914|76884197	Reep6	mmu-miR-345-5p, mmu-miR-664-5p	0.68	0.022
2:76857904|76888087	Snta1	mmu-miR-345-5p, mmu-miR-664-5p	0.74	0.012
2:76859914|76884197	Tsc1	mmu-miR-345-5p, mmu-miR-664-5p	0.60	0.045
2:76857904|76888087	Csdc2	mmu-miR-345-5p, mmu-miR-664-5p	0.80	0.005
2:76850570|76884197	Csdc2	mmu-miR-345-5p, mmu-miR-664-5p	0.59	0.046
2:76859914|76884197	Csdc2	mmu-miR-345-5p, mmu-miR-664-5p	0.90	0.000
2:76857904|76888087	Pfkfb3	mmu-miR-345-5p, mmu-miR-708-5p	0.64	0.032
2:76857904|76888087	Pcyt1a	mmu-miR-345-5p, mmu-miR-708-5p	0.61	0.041
2:76857904|76888087	Tead1	mmu-miR-345-5p, mmu-miR-708-5p	0.79	0.006
2:76857904|76888087	Map3k13	mmu-miR-345-5p, mmu-miR-708-5p	0.68	0.023
7:90160448|90197020	Gpd2	mmu-miR-483-5p	0.74	0.012
7:90160448|90197020	Afg3l1	mmu-miR-483-5p	0.60	0.043
19:42562552|42583543	Eif5a	mmu-miR-664-5p	0.62	0.037
2:76857904|76888087	Add1	mmu-miR-664-5p	0.60	0.044
2:76850570|76884197	Add1	mmu-miR-664-5p	0.67	0.024
19:42562552|42583543	Zer1	mmu-miR-664-5p	0.63	0.035
2:76857904|76888087	Zer1	mmu-miR-664-5p	0.76	0.009
2:76850570|76884197	Zer1	mmu-miR-664-5p	0.62	0.039
19:42562552|42583543	Prokr1	mmu-miR-664-5p	0.89	0.001
2:76857904|76888087	Prokr1	mmu-miR-664-5p	0.62	0.039
2:76859914|76884197	Prokr1	mmu-miR-664-5p	0.61	0.040
2:76857904|76888087	Mbnl2	mmu-miR-664-5p	0.80	0.005

(*continued on next page*)

Table 4 (*continued*)

circRNA	mRNA	Shared miRNAs	ceRNA score	*P*-value
2:76859914|76884197	Mbnl2	mmu-miR-664-5p	0.62	0.038
19:42562552|42583543	9530068E07Rik	mmu-miR-664-5p	0.62	0.039
2:76850570|76884197	Rnf114	mmu-miR-664-5p	0.59	0.047
2:76850570|76884197	Grin3a	mmu-miR-664-5p	0.67	0.024
19:42562552|42583543	Reep6	mmu-miR-664-5p	0.61	0.040
19:42562552|42583543	Sh3kbp1	mmu-miR-664-5p	0.59	0.047
2:76857904|76888087	Sh3kbp1	mmu-miR-664-5p	0.68	0.023
2:76850570|76884197	Sh3kbp1	mmu-miR-664-5p	0.70	0.018
2:76857904|76888087	Tom1l2	mmu-miR-664-5p	0.60	0.044
2:76859914|76884197	Trpc6	mmu-miR-664-5p	0.62	0.039
2:76857904|76888087	Galns	mmu-miR-664-5p	0.70	0.017
2:76850570|76884197	Fgf11	mmu-miR-664-5p	0.69	0.019
2:76850570|76884197	Rnf146	mmu-miR-664-5p	0.64	0.031
2:76857904|76888087	Bcl7b	mmu-miR-664-5p	0.89	0.001
2:76850570|76884197	Bcl7b	mmu-miR-664-5p	0.64	0.032
2:76859914|76884197	Bcl7b	mmu-miR-664-5p	0.73	0.014
2:76859914|76884197	Arrb1	mmu-miR-664-5p	0.76	0.009
19:42562552|42583543	Mapre2	mmu-miR-664-5p	0.59	0.049
2:76850570|76884197	Mapre2	mmu-miR-664-5p	0.87	0.001
19:42562552|42583543	Plekhm2	mmu-miR-664-5p	0.62	0.038
2:76850570|76884197	Ccp110	mmu-miR-664-5p	0.74	0.011
19:42562552|42583543	Ppp6r3	mmu-miR-664-5p	0.95	0.000
2:76857904|76888087	Ppp6r3	mmu-miR-664-5p	0.78	0.006
2:76850570|76884197	Ppp6r3	mmu-miR-664-5p	0.67	0.024
2:76859914|76884197	Ppp6r3	mmu-miR-664-5p	0.68	0.022
2:76859914|76884197	Tom1l2	mmu-miR-664-5p	0.60	0.045
2:76857904|76888087	Bcl9l	mmu-miR-664-5p	0.68	0.022
2:76859914|76884197	Bcl9l	mmu-miR-664-5p	0.64	0.032
19:42562552|42583543	Csdc2	mmu-miR-664-5p	0.73	0.013
19:42562552|42583543	Wipf3	mmu-miR-664-5p	0.87	0.001
2:76857904|76888087	Wipf3	mmu-miR-664-5p	0.90	0.000
2:76850570|76884197	Wipf3	mmu-miR-664-5p	0.65	0.029
2:76859914|76884197	Wipf3	mmu-miR-664-5p	0.77	0.008
2:76850570|76884197	Spr	mmu-miR-664-5p	0.59	0.048
2:76857904|76888087	Lemd2	mmu-miR-664-5p	0.78	0.007
2:76850570|76884197	Lemd2	mmu-miR-664-5p	0.58	0.049
2:76859914|76884197	Lemd2	mmu-miR-664-5p	0.66	0.027
2:76859914|76884197	Eif5a	mmu-miR-664-5p	0.71	0.017
19:42562552|42583543	Kmt5b	mmu-miR-664-5p	0.66	0.027
19:42562552|42583543	Tnip1	mmu-miR-664-5p	0.66	0.027
2:76857904|76888087	Tnip1	mmu-miR-664-5p	0.74	0.011
2:76859914|76884197	Tnip1	mmu-miR-664-5p	0.86	0.002
19:42562552|42583543	Ppp6r3	mmu-miR-664-5p	0.90	0.000
2:76857904|76888087	Ppp6r3	mmu-miR-664-5p	0.59	0.048
2:76857904|76888087	Golga1	mmu-miR-664-5p, mmu-miR-708-5p	0.76	0.009
2:76857904|76888087	Syngr2	mmu-miR-708-5p	0.70	0.018
2:76857904|76888087	Fblim1	mmu-miR-708-5p	0.75	0.009
2:76857904|76888087	Ddx11	mmu-miR-708-5p	0.81	0.004
2:76857904|76888087	Rab22a	mmu-miR-708-5p	0.70	0.017
2:76857904|76888087	Atg9a	mmu-miR-708-5p	0.61	0.040
2:76857904|76888087	Clmn	mmu-miR-708-5p	0.89	0.001
2:76857904|76888087	Supt7l	mmu-miR-708-5p	0.62	0.036
2:76857904|76888087	Adgrl3	mmu-miR-708-5p	0.60	0.043
2:76857904|76888087	Syngr2	mmu-miR-708-5p	0.80	0.005

we screened serve as indicative markers of differentially expressed dysfunctional ncRNAs associated with TIC.

The ceRNA network has been described as a complex post-transcriptional endogenous regulatory network in which circRNAs, lncRNAs, and other RNAs act as sponges for miRNAs to regulate mRNA expression [32]. Extensive research substantiates that ceRNA activity orchestrates a comprehensive regulatory framework within the transcriptome, significantly augmenting the functional genetic landscape in the human genome and playing a pivotal role in various pathological conditions, notably cardiovascular diseases [33,34]. We propose that the DEGs screened by whole-transcriptome RNA seq will play a critical regulatory function in TIC by participating in ceRNA networks. Consequently, we constructed a both circRNA-related ceRNA network and a lncRNA-related ceRNA network, containing 7 circRNAs, 43 lncRNAs, 10 miRNAs, and 133 mRNAs.

Each RNA was evaluated for centrality using Cytoscape's CytoNCA plugin to identify core genes. The analysis revealed that miR-31-5p attained the highest degree, scoring 53, within lncRNA-associated ceRNA networks. Numerous studies have underscored the involvement of miR-31-5p in cancer, cardiovascular diseases, and other pathological conditions [35]. Most importantly, Xiaoyu Ji et al. found that miR-31-5p alleviates doxorubicin-induced cardiotoxicity through the interaction with quaking circRNA Pan3, but its role in TIC is unclear [36]. Similarly, miR-664-5p was found to have the highest score of 35 in circRNA-associated ceRNA networks. Bo Sun et al. found miR-644-5p, carried by bone mesenchymal stem cell-derived exosomes, targeting p53 regulation to inhibit ovarian granulosa cell apoptosis [37]. Studies have also indicated that miR-664-5p promotes myoblast proliferation while inhibiting myoblast differentiation [38]. Notably, the potential role of miR-31-5p and miR-644-5p in TIC have not been previously reported, warranting further investigation in our subsequent studies.

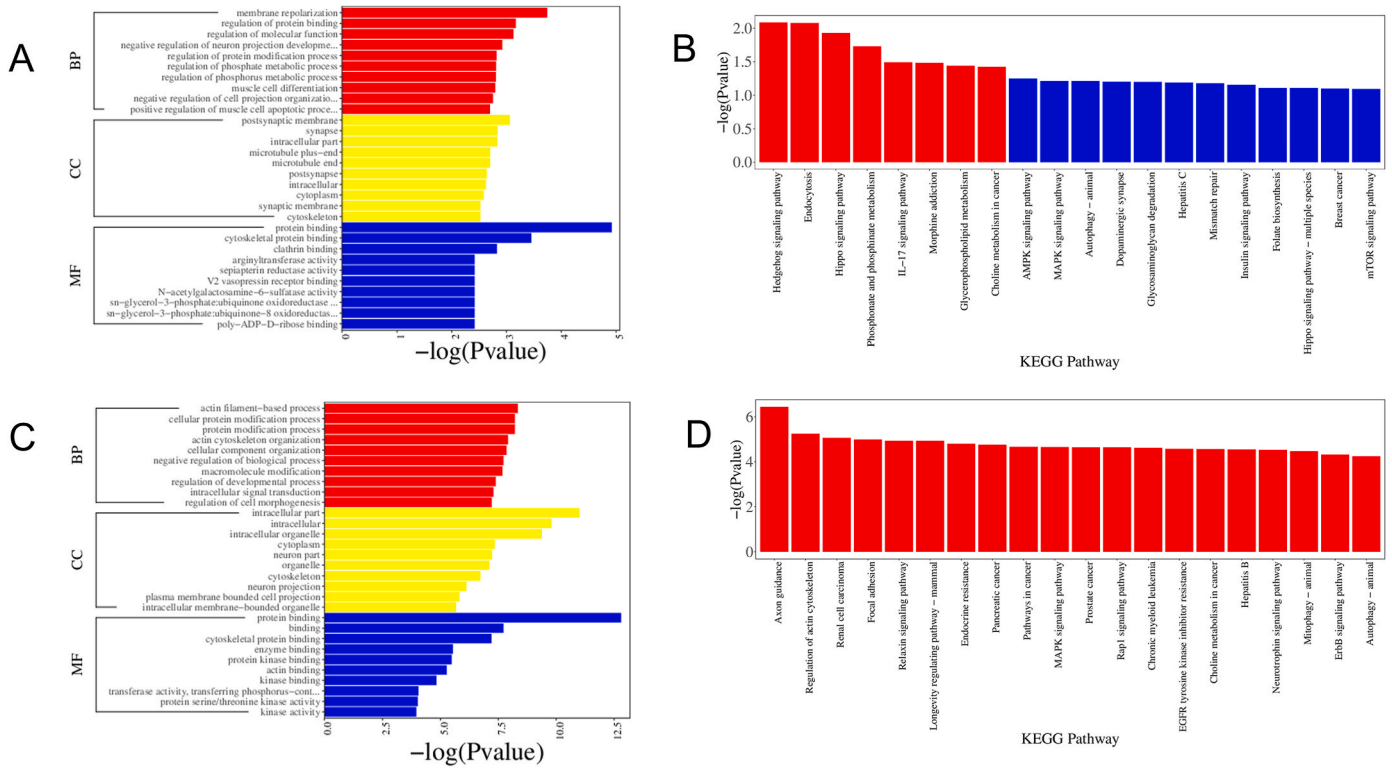

Fig. 6. Bioinformatic analysis of the ceRNA network. Data of bioinformatic analysis in the circRNA-associated ceRNA network with GO (A) and KEGG (B) pathway analysis, and in the lncRNA-associated ceRNA network with GO (C) and KEGG (D) pathway analysis (n = 3). GO, Gene Ontology; KEGG, Kyoto Encyclopedia of Genes and Genomes.

Through GO and KEGG analyses, we further analyzed the pathways and functions in which the ceRNA networks are involved in. GO analysis indicated that these networks are involved in "protein modification process" and "regulation of molecular function", among other life processes. According to the KEGG enrichment results, "Hippo signaling pathway" and "MAPK signaling pathway" were enriched in the circRNA-associated ceRNA and lncRNA-associated ceRNA networks, respectively. The Hippo signaling pathway is a signaling pathway that inhibits cell proliferation [39]. Recent research has confirmed that the Hippo signaling pathway is also involved in cancer development and metastasis, tissue regeneration, and functional regulation of stem cells [40].

NcRNA-mRNA interaction stands out as one of the most extensively explored molecular mechanisms of ncRNA [41]. To scrutinize the interaction and regulatory dynamics among the DEGs, we have devised a co-expression network. Within this network, mmu-miR-33-5p and ENSMUST00000190825 (Rbbp5) attain the highest scores, indicative of their pivotal roles in the network framework. Changes in their expression levels emerge as pivotal factors influencing alterations in the expression patterns of other RNAs within the network. Presently, there is a dearth of literature examining mmu-miR-33-5p. Conversely, Rbbp5 is commonly perceived as a risk factor, exhibiting elevated levels in diabetic cardiomyopathy, with increased expression linked to embryonic lethality in mice [42,43]. Our research findings substantiate these associations; in the TIC model we constructed, Rbbp5 expression is likewise upregulated.

Certainly, beyond the previously mentioned mechanisms, ncRNA plays a crucial role in cellular regulation through processes like modulating alternative splicing and transcriptional regulation. Certain circRNAs exhibit the ability to interact with transcription factors, thereby impacting their binding efficiency on chromatin and subsequently regulating the transcription of target genes. This mode of action significantly influences the activity of gene promoters, thereby finely tuning gene expression levels [44]. Moreover, circRNAs may contribute to the modulation of the three-dimensional structure of chromatin by engaging in interactions with it, consequently affecting the epigenetic modifications of genes, including methylation and acetylation of histones. Throughout the processing of original RNA molecules, splicing enzymes possess the capability to selectively excise different exons, leading to the creation of multiple mRNA isoforms. In this intricate process, ncRNA can interact with splicing complexes, thereby influencing the diversity of gene products. Alternative splicing stands out as a pivotal regulatory mechanism capable of generating various protein isoforms from a single gene, ultimately enhancing the functional diversity of genes [45].

5. Conclusion

We screened 43 circRNAs, 270 lncRNAs, 12 miRNAs, and 4131 mRNAs by whole-transcriptome RNA sequencing. Subsequently, we constructed a circRNA-associated ceRNA network, a lncRNA-associated ceRNA network, a co-expression network, and an RNA-RBP network. We identified some core RNAs based on these networks which have potential roles in the treatment of TIC, and we will next investigate their roles in TIC.

Funding

This study was supported by grants of the National Natural Scientific Foundation of China (Nos. 82173911, 82373970, 81973406), Fundamental Research Funds for the Central Universities of Central South University (Nos. 2022ZZTS0954, 2023ZZTS0891), Hunan Provincial Natural Scientific Foundation (Nos. 2019JJ50849, 2020JJ4823, 2022JJ80109), Scientific Research Project of Hunan Provincial Health and Family Planning Commission (No. 202113050843), Research Project established by Chinese Pharmaceutical Association Hospital Pharmacy department (No. CPA-Z05-ZC-2021-002), Hunan Provincial

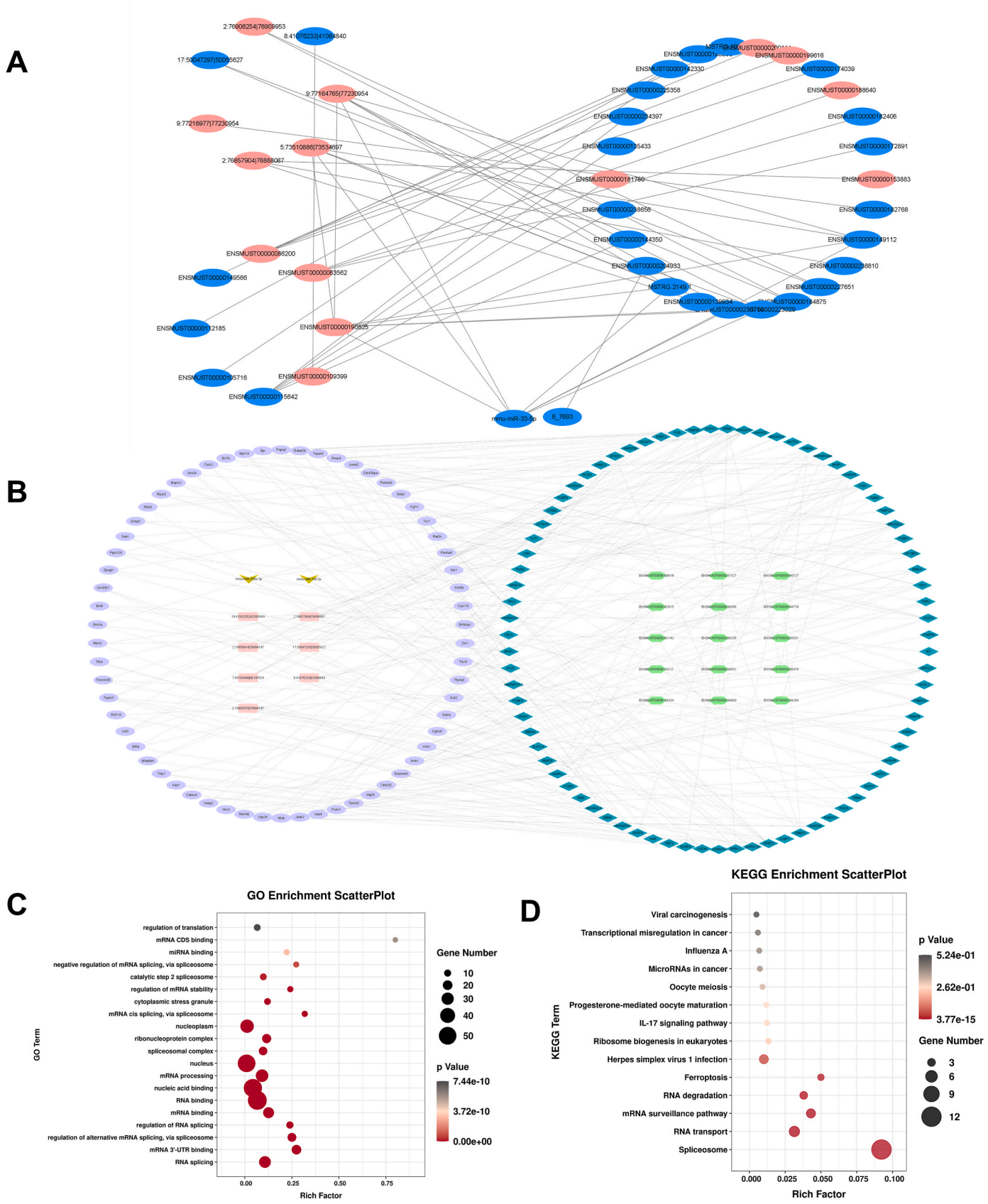

Fig. 7. co-expression network and RNA-RBP network. (A) The co-expression network between DEGs. The same type of RNA forms a circle. Red represents upregulated; blue represents downregulated. (B) The RNA-RBP network of the DEGs in the subnetwork of circRNAs/lncRNAs associated ceRNA network. (C) The GO Enrichment of RBPs. (D) The KEGG Enrichment of RBPs.

Innovation Foundation for Postgraduate (No. CX20230324), Fundamental Research Funds for the Central Universities of Central South University (No. 2023ZZTS0252).

Availability of data and material

The authors can confirm that all relevant data are included in the article which are open and transparent.

Ethics approval

The experimental designs and animal care were conducted in accordance with the Guide for the Care and Use of Laboratory Animals, published by the National Institutes of Health (NIH Publication No. 85–23, revised 1996) and approved by the Xiangya Medical College of Central South University.

CRediT authorship contribution statement

Suifen Xie: Writing – original draft, Investigation. **Ni Zhou:** Writing – original draft, Investigation. **Nan Su:** Investigation. **Zijun Xiao:** Methodology. **Shanshan Wei:** Supervision, Methodology. **Yuanying Yang:** Supervision. **Jian Liu:** Resources. **Wenqun Li:** Writing – review & editing, Funding acquisition. **Bikui Zhang:** Writing – review & editing, Funding acquisition.

Declaration of competing interest

The authors declare that they have no competing interests.

Appendix A. Supplementary data

Supplementary data to this article can be found online at https://doi.org/10.1016/j.ncrna.2024.02.004.

References

[1] A.M. Mousa, et al., Could allicin alleviate trastuzumab-induced cardiotoxicity in a rat model through antioxidant, anti-inflammatory, and antihyperlipidemic properties? Life Sci. 302 (May 21 2022) 120656 https://doi.org/10.1016/j.lfs.2022.120656 (in eng).
[2] J. Jiang, B. Liu, S.S. Hothi, Herceptin-mediated cardiotoxicity: assessment by cardiovascular magnetic resonance, Cardiol. Res. Pract. 2022 (2022) 1910841, https://doi.org/10.1155/2022/1910841 (in eng).
[3] R. Madonna, et al., Improving the preclinical models for the study of chemotherapy-induced cardiotoxicity: a position paper of the Italian working group on drug cardiotoxicity and cardioprotection, Heart Fail. Rev. 20 (5) (Sep 2015) 621–631, https://doi.org/10.1007/s10741-015-9497-4 (in eng).
[4] M.S. Ewer, S.M. Lippman, Type II chemotherapy-related cardiac dysfunction: time to recognize a new entity, J. Clin. Oncol. 23 (13) (May 1 2005) 2900–2902, https://doi.org/10.1200/jco.2005.05.827 (in eng).
[5] N. Dempsey, A. Rosenthal, N. Dabas, Y. Kropotova, M. Lippman, N.H. Bishopric, Trastuzumab-induced cardiotoxicity: a review of clinical risk factors, pharmacologic prevention, and cardiotoxicity of other HER2-directed therapies, Breast Cancer Res. Treat. 188 (1) (Jul 2021) 21–36, https://doi.org/10.1007/s10549-021-06280-x (in eng).
[6] I. Zhang, A. Barac, Cardioprotection for anti-HER2 therapy: considerations for primary prevention and use in mildly reduced left ventricular ejection fraction, Curr. Oncol. Rep. 24 (8) (Aug 2022) 1063–1070, https://doi.org/10.1007/s11912-022-01234-y, in eng.
[7] S. Hombach, M. Kretz, Non-coding RNAs: classification, biology and functioning, Adv. Exp. Med. Biol. 937 (2016) 3–17, https://doi.org/10.1007/978-3-319-42059-2_1 (in eng).
[8] E. Huntzinger, E. Izaurralde, Gene silencing by microRNAs: contributions of translational repression and mRNA decay, Nat. Rev. Genet. 12 (2) (Feb 2011) 99–110, https://doi.org/10.1038/nrg2936 (in eng).
[9] A.C. Panda, Circular RNAs act as miRNA sponges, Adv. Exp. Med. Biol. 1087 (2018) 67–79, https://doi.org/10.1007/978-981-13-1426-1_6 (in eng).
[10] A. Jusic, et al., Noncoding RNAs in age-related cardiovascular diseases, Ageing Res. Rev. 77 (May 2022) 101610, https://doi.org/10.1016/j.arr.2022.101610 (in eng).
[11] P. Ginckels, P. Holvoet, Oxidative stress and inflammation in cardiovascular diseases and cancer: role of non-coding RNAs, in: eng (Ed.), Yale J. Biol. Med. 95 (1) (Mar 2022) 129–152.
[12] X.D. Fu, Non-coding RNA: a new frontier in regulatory biology, Natl. Sci. Rev. 1 (2) (Jun 1 2014) 190–204, https://doi.org/10.1093/nsr/nwu008, in eng.
[13] H. Liu, et al., Longitude variation of the microRNA-497/FGF-23 Axis during treatment and its linkage with neoadjuvant/adjuvant trastuzumab-induced cardiotoxicity in HER2-positive breast cancer patients, Front Surg 9 (2022) 862617, https://doi.org/10.3389/fsurg.2022.862617 in eng.
[14] M. Lunardi, et al., Genetic and RNA-related molecular markers of trastuzumab-chemotherapy-associated cardiotoxicity in HER2 positive breast cancer: a systematic review, BMC Cancer 22 (1) (Apr 12 2022) 396, https://doi.org/10.1186/s12885-022-09437-z, in eng.
[15] J. Li, L. Li, X. Li, S. Wu, Long noncoding RNA LINC00339 aggravates doxorubicin-induced cardiomyocyte apoptosis by targeting MiR-484, Biochem. Biophys. Res. Commun. 503 (4) (Sep 18 2018) 3038–3043, https://doi.org/10.1016/j.bbrc.2018.08.090, in eng.
[16] R.S. Zhou, et al., Integrated analysis of lncRNA-miRNA-mRNA ceRNA network in squamous cell carcinoma of tongue, BMC Cancer 19 (1) (Aug 7 2019) 779, https://doi.org/10.1186/s12885-019-5983-8, in eng.
[17] D.L. Cheng, Y.Y. Xiang, L.J. Ji, X.J. Lu, Competing endogenous RNA interplay in cancer: mechanism, methodology, and perspectives, Tumour Biol 36 (2) (Feb 2015) 479–488, https://doi.org/10.1007/s13277-015-3093-z, in eng.
[18] G. Milano, et al., Intravenous administration of cardiac progenitor cell-derived exosomes protects against doxorubicin/trastuzumab-induced cardiac toxicity, Cardiovasc. Res. 116 (2) (Feb 1 2020) 383–392, https://doi.org/10.1093/cvr/cvz108, in eng.
[19] C. Kasavi, Gene co-expression network analysis revealed novel biomarkers for ovarian cancer, Front. Genet. 13 (2022) 971845, https://doi.org/10.3389/fgene.2022.971845 (in eng).
[20] Y. Mao, Q. Nie, Y. Yang, G. Mao, Identification of co-expression modules and hub genes of retinoblastoma via co-expression analysis and protein-protein interaction networks, Mol. Med. Rep. 22 (2) (Aug 2020) 1155–1168, https://doi.org/10.3892/mmr.2020.11189, in eng.
[21] M. Kori, E. Gov, K.Y. Arga, Novel genomic biomarker candidates for cervical cancer as identified by differential Co-expression network analysis, OMICS 23 (5) (May 2019) 261–273, https://doi.org/10.1089/omi.2019.0025 (in eng).
[22] D.L. Shi, RNA-binding proteins as critical post-transcriptional regulators of cardiac regeneration, Int. J. Mol. Sci. 24 (15) (Jul 26 2023), https://doi.org/10.3390/ijms241512004 in eng.
[23] S. Paz, A. Ritchie, C. Mauer, M. Caputi, The RNA binding protein SRSF1 is a master switch of gene expression and regulation in the immune system, Cytokine Growth Factor Rev. 57 (Feb 2021) 19–26, https://doi.org/10.1016/j.cytogfr.2020.10.008 (in eng).
[24] P. Zhong, J. Peng, M. Yuan, B. Kong, H. Huang, Cold-inducible RNA-binding protein (CIRP) in inflammatory diseases: molecular insights of its associated signalling pathways, Scand. J. Immunol. 93 (1) (Jan 2021) e12949, https://doi.org/10.1111/sji.12949 in eng.
[25] P. Bielli, R. Busà, M.P. Paronetto, C. Sette, The RNA-binding protein Sam68 is a multifunctional player in human cancer, Endocr. Relat. Cancer 18 (4) (Aug 2011) R91–r102, https://doi.org/10.1530/erc-11-0041 (in eng).
[26] Y. Yu, W. Zhang, D. Zhu, H. Wang, H. Shao, Y. Zhang, LncRNA Rian ameliorates sevoflurane anesthesia-induced cognitive dysfunction through regulation of miR-143-3p/LIMK1 axis, Hum. Cell 34 (3) (May 2021) 808–818, https://doi.org/10.1007/s13577-021-00502-6 (in eng).
[27] D.J. Slamon, et al., Use of chemotherapy plus a monoclonal antibody against HER2 for metastatic breast cancer that overexpresses HER2, N. Engl. J. Med. 344 (11) (Mar 15 2001) 783–792, https://doi.org/10.1056/nejm200103153441101, in eng.
[28] W. Poller, et al., Non-coding RNAs in cardiovascular diseases: diagnostic and therapeutic perspectives, Eur. Heart J. 39 (29) (Aug 1 2018) 2704–2716, https://doi.org/10.1093/eurheartj/ehx165, in eng.
[29] Y. Wang, et al., 1, 8-cineole attenuates cardiac hypertrophy in heart failure by inhibiting the miR-206-3p/SERP1 pathway, Phytomedicine 91 (Oct 2021) 153672, https://doi.org/10.1016/j.phymed.2021.153672 (in eng).
[30] Z. Song, et al., Overexpression of MFN2 alleviates sorafenib-induced cardiomyocyte necroptosis via the MAM-CaMKIIδ pathway in vitro and in vivo, Theranostics 12 (3) (2022) 1267–1285, https://doi.org/10.7150/thno.65716 (in eng).
[31] Y. Chen, et al., Isorhapontigenin attenuates cardiac microvascular injury in diabetes via the inhibition of mitochondria-associated ferroptosis through PRDX2-MFN2-ACSL4 pathways, Diabetes 72 (3) (Mar 1 2023) 389–404, https://doi.org/10.2337/db22-0553 (in eng).
[32] Y. Yang, et al., lncRNA ZFAS1 promotes lung fibroblast-to-myofibroblast transition and ferroptosis via functioning as a ceRNA through miR-150-5p/SLC38A1 axis, Aging (Albany NY) 12 (10) (May 26 2020) 9085–9102, https://doi.org/10.18632/aging.103176, in eng.
[33] X. Gu, et al., Comprehensive circRNA expression profile and construction of circRNA-related ceRNA network in cardiac fibrosis, in: eng (Ed.), Biomed. Pharmacother. 125 (May 2020) 109944, https://doi.org/10.1016/j.biopha.2020.109944.
[34] L. Salmena, L. Poliseno, Y. Tay, L. Kats, P.P. Pandolfi, A ceRNA hypothesis: the Rosetta Stone of a hidden RNA language? Cell 146 (3) (Aug 5 2011) 353–358, https://doi.org/10.1016/j.cell.2011.07.014, in eng.
[35] K. Yang, et al., Prevention of aortic dissection and aneurysm via an ALDH2-mediated switch in vascular smooth muscle cell phenotype, Eur. Heart J. 41 (26) (Jul 7 2020) 2442–2453, https://doi.org/10.1093/eurheartj/ehaa352, in eng.
[36] X. Ji, et al., MicroRNA-31-5p attenuates doxorubicin-induced cardiotoxicity via quaking and circular RNA Pan3, J. Mol. Cell. Cardiol. 140 (Mar 2020) 56–67, https://doi.org/10.1016/j.yjmcc.2020.02.009, in eng.
[37] B. Sun, Y. Ma, F. Wang, L. Hu, Y. Sun, miR-644-5p carried by bone mesenchymal stem cell-derived exosomes targets regulation of p53 to inhibit ovarian granulosa

cell apoptosis, Stem Cell Res. Ther. 10 (1) (Nov 29 2019) 360, https://doi.org/10.1186/s13287-019-1442-3, in eng.
[38] R. Cai, et al., MicroRNA-664-5p promotes myoblast proliferation and inhibits myoblast differentiation by targeting serum response factor and Wnt1, J. Biol. Chem. 293 (50) (Dec 14 2018) 19177–19190, https://doi.org/10.1074/jbc.RA118.003198, in eng.
[39] S. Ma, Z. Meng, R. Chen, K.L. Guan, The hippo pathway: biology and pathophysiology, Annu. Rev. Biochem. 88 (Jun 20 2019) 577–604, https://doi.org/10.1146/annurev-biochem-013118-111829, in eng.
[40] A. Dey, X. Varelas, K.L. Guan, Targeting the Hippo pathway in cancer, fibrosis, wound healing and regenerative medicine, Nat. Rev. Drug Discov. 19 (7) (Jul 2020) 480–494, https://doi.org/10.1038/s41573-020-0070-z, in eng.
[41] X. Li, J. Li, G. Shan, X. Wang, Identification of long non-coding RNA and circular RNA associated networks in cellular stress responses, Front. Genet. 14 (2023) 1097571, https://doi.org/10.3389/fgene.2023.1097571 in eng.
[42] V. Malek, N. Sharma, A.B. Gaikwad, Simultaneous inhibition of neprilysin and activation of ACE2 prevented diabetic cardiomyopathy, Pharmacol. Rep. 71 (5) (Oct 2019) 958–967, https://doi.org/10.1016/j.pharep.2019.05.008, in eng.
[43] H. Zhong, et al., c-JUN is a barrier in hESC to cardiomyocyte transition, Life Sci. Alliance 6 (11) (Nov 2023), https://doi.org/10.26508/lsa.202302121 in eng.
[44] Z. Li, et al., Exon-intron circular RNAs regulate transcription in the nucleus, Nat. Struct. Mol. Biol. 22 (3) (Mar 2015) 256–264, https://doi.org/10.1038/nsmb.2959, in eng.
[45] X. Wang, et al., CircURI1 interacts with hnRNPM to inhibit metastasis by modulating alternative splicing in gastric cancer, Proc. Natl. Acad. Sci. U. S. A. 118 (33) (Aug 17 2021), https://doi.org/10.1073/pnas.2012881118 in eng.